Characterization of Short-Term Wind Power Variations and Estimation of Reserve Requirements for High Wind Generation Shares

M. Saber Eltohamy[1,], M. Said Abdel Moteleb[2], Hossam E. A. Talaat[3], S. F. Mekhamer[4], Walid Omran[5]

[1,2]Dept. of Power Electronics and Energy Conversion, Electronics Research Institute, Egypt
[1]Electrical Power and Machines Engineering Department, Faculty of Engineering, Ain Shams University, Cairo, Egypt
[3,4]Department of Electrical Engineering, Future University in Egypt, Egypt
[5]Department of Mechatronics, Faculty of Engineering and Materials Science, German University in Cairo, Egypt

Article Info	ABSTRACT
	The need to deal with variability in wind power output is one of the greatest challenges connected with adopting a considerable amount of wind power into power grids. Power system operators need to acquire more information on this variability, which can be utilized in the mitigation of high ramping events, especially when these events synchronize with a large error in the prediction, ensuring flexibility and reliability in the power system besides the economic considerations. The paper analyses short-term variability in output power using actual data obtained from aggregated wind farms from 2015 to 2020, where power ramping characteristics are described using a variety of measurements. The use of the standard deviation of short-term wind power variation as a reserve measure will be investigated in detail since there is no consensus about the ideal confidence level value as a multiplier of σ, which ranges from 3 to 6 times σ. The paper addresses how large this confidence level should be, as well as developing a data-driven approach for estimating this reserve with increasing wind shares and evaluating the proper distribution of short-term wind variation. The results illustrate that the stochastic variations in wind power can retain many of their characteristics from year to year, even when the share of wind capacity is raised.

Corresponding Author:

M. Saber Eltohamy,
Department of Power Electronics and Energy Conversion,
Electronics Research Institute, Egypt
Email: Electronics Research Institute, Egypt

1.   INTRODUCTION

Power systems are steadily increasing generation from renewable resources at the expense of fossil fuels to diversify generating supplies for improved reliability while also meeting environmental targets [1][2]. Hence, renewable generation (RG) accounted for 82% of total capacity increases in 2020, and wind and solar generating represented 91% of that [3]. Another remarkable fact worth considering is the response of wind energy in the face of exceptional times such as COVID-19 pandemic and the current war between Russia and Ukraine, as the fossil fuels sector during these events experienced market volatility, whereas the wind energy sector exhibited a more stable response [4][5]. However, RG increases energy variability and uncertainty [6], since its production changes based on climatic conditions. Thus, power system planners are looking for flexible generating sources that support renewable instead of just looking for sources of generation to meet demand [7][8].

Studying RG variability is essential to system operators [9][10], who should study, analyse, and take the required measures to avoid the consequences of high power ramping occurrences [11][12]. In [13], the authors quantify the ranges of wind power output, only 3 months of data are utilised to construct dynamic

ranges, whilst wind variations vary with seasons, and times of the day [14], therefore further data would contain additional information and could produce different ranges [15]. The investigation of increasing shares of variable RG on the characteristics of power ramping has been discussed in [16][17] through statistical analysis of historical data. In [18][19], new metrics have been introduced for understanding the characteristics of power ramping. In [20], the ramp rates of in-stream tidal, solar, and wind as uncorrelated RGs have been investigated to optimise their capacity combination. The authors of [21] evaluated the level of complementarity of wind, PV, and hydro-power by studying variability and ramp events, they showed that the combined PV–wind power production has a better performance for offsetting the ramp events, and the wind power fluctuates more violently than PV. Analysis of wind power in shorter periods showed more variability and resulted in an improved cost estimation [22]. The authors of [23] showed the relevance of distance among wind farms on the variability of power output. Distributing wind farms over a larger area decreases the effects of diurnal and synoptic wind peaks because changeable weather patterns do not affect each turbine at the same time [12][24]. While all predictive algorithms in [25] predicted just a few ramp events, future studies should incorporate ramp forecasts of RG [26], as the prediction error rate is still rather high [27][28], and influences the balance of generation and demand [29][30], which impacts electricity prices [31]. In [32], the authors enhanced long short term memory to increase the accuracy of the wind power forecast. The wind power signal exhibits great unpredictability, while the wind power data exhibit long-term correlation. Belgium's 2018 wind power data was used to test the forecasting technique, the ramp prediction was not totally solved, and the forecast error remained considerable when ramp events occurred, although it was far smaller than other forecast approaches. The authors demonstrated that the pattern of ramp events is too complex to identify with accuracy, making it difficult for future research to identify patterns related to ramp events. So, improving the methods of forecasting is still under investigation [33][34]. The link between the weather mechanisms and ramp events has been studied, trying to investigate the weather mechanisms that create upward and downward ramp events [35][36], although it is an extremely case-dependent problem [37][38]. In [25], just 34% of ramp events had their causes identified, while no explanation was made for the remaining proportion. Wind power has more intermittency than the wind speed that produced it [24][10]. Therefore, the fluctuations linked with the wind speed forecasts are lower than that observed, and wind speed alone cannot explain a large percentage of wind power fluctuations [39].

In [40], the reserve associated with wind generation was estimated, and this reserve increased linearly with regard to the wind penetration rate. In [41][42], the geo-spreading of wind farms has a smoothing impact on the inherent variations, hence linear upscaling of the reserve with expansion in wind generation should be avoided [43]. The operation of power systems is based on probabilities and risks, so reserves are generally estimated to cover fluctuations within a certain probability [44]. Recently, most approaches in the calculation of reserves have moved toward probabilistic methodologies [45][46]. In [47], the stochastic and deterministic models have been compared to represent the short-term fluctuation of wind and solar power in a European long-term least-cost optimization model that is used to address investments for the interconnected European nations into 2050. Investigating how various approaches to account for uncertainty and various temporal resolutions affect model outcomes is part of this. Representative days or time slices were used to express the temporal resolution. Six years of hourly load data were utilized, with the assumption that the load profile in 2050 will have the same shape and thirty years of historical hourly capacity factors of combined wind and solar power were used to reflect short-term variability. Stochastic models have been suggested as an alternative to deterministic models for long-term studies involving large shares of variable renewable energy sources. This is because deterministic models base investment decisions on a single operational scenario, while stochastic models consider a variety of representative operational scenarios that may arise.

The reserve needs were calculated in [48] based on the distribution of wind power variations. Load and short-term PV variations were assumed to be based on normal distribution, whereas other distributions were thought to be more precise for wind data [43], such as Weibull, Gamma, and Laplace [42][48][49]. While using different definitions to estimate wind power fluctuations in [50], affected the obtained distributions. Previously conducted studies also assumed that the probability density function of wind power variations is invariant, which was not supported by evidence. Wind variations and uncertainty are not normally distributed [51][52]. Furthermore, the central-limit theorem, which predicts the convergence to the normal distribution, did not apply in [12]. In the case of normal distribution, adjusting the reserve at three standard deviations (3σ) of the mean will absorb 99.7% of imbalances but the variations in wind power followed a normal distribution with longer tails [50], requiring more reserve to be absorbed [53][54]. The authors of [55] computed how many times the standard deviation value of the hourly variations and minute-to-minute fluctuations should be multiplied to get the 99.7% percentile value, they found that the standard deviation values have to be multiplied by about 5.6 to obtain the regulations calculated by the percentile value, and by around 3.4 to reach the load following determined by the percentile value. In contrast, the optimal confidence level in [41] was 3σ. The additional variability of wind was estimated to be a 2 MW standard deviation with each 100 MW wind farm

erected according to the operational data from wind farms, and the standard deviation multiplier was assumed to be 5 in the calculation of the regulating reserve required [56].

Determining extra operational reserves is a significant concern in power systems that target considerable wind penetration. For the same wind penetration level, the divergence in the estimated reserve sizes is attributed in [57] [58] to differences in reserve sizing methods utilized in different research. There is no common approach for calculating reserve requirements [59], so the question of how to estimate the required reserves to accommodate short-term variations at different wind power penetration levels is still open. The effects of wind variability on operational reserves are most noticeable in the time range of 10–15 minutes [41][60], therefore having a significant impact on secondary power reserves [43]. The dispatch captures variability over larger time scales than the dispatch period, therefore reserves must only cover variability during the dispatch period [59]. To overcome this issue, this paper proposes an improved reserve estimation methodology. The standard deviation multiplier is used to cover almost every incidence of wind fluctuation with a given degree of certainty. After performing a long-term analysis of short-term variations in wind generation with increasing penetration over five years, using various metrics from [18][19], the historical data available are used to create secure operating reserves since longer data sets with higher quality are essential to provide far more detail about the expected variations in wind power [61][16]. In addition, the best-fitted probability distribution function (PDF) to short-term wind variations will be studied, as it is more important than ever to model this variability with increasing shares of wind generation. The basic goals and structure of this paper are as follows: In Section 2, the paper begins with an overview of the characteristics of power ramps and the metrics used in measuring wind power variations, before applying these metrics to a practical case described in this section using real data recorded from aggregated wind farms between 2015 and 2020. This section also demonstrates the advantages of the probabilistic/statistical method over the other methods in reserve estimations. Second, in Section 3, the paper discusses the results of studying short-term variations, as well as modelling these variations by fitting various probability distribution functions (PDFs) to get the best-fitted one. In addition, the paper proposes a method for estimating the required reserve at different confidence levels using the standard deviation multiplier for these variations, and the estimated reserves are evaluated. Finally, in Section 4, the paper summarizes the major findings and highlights the contribution.

2.   POWER RAMPS

2.1. Characteristics of Power Ramps

The power ramps may be up or down, and the ramp is defined as a ramp event when it has a sharp change in power within a short time scale [62], and the threshold value of its magnitude is selected to reveal the magnitude of power change at a defined time interval, which is hard to manage and can lead to grave problems in the next few hours or days [63], so it is user-defined based on the system operators' input [64] and is therefore differing between power systems [11]. The magnitude of ramp event is generally indicated for wind generation as a proportion of installed capacity or in megawatts. The time interval (Δt) used to identify the ramp in minutes/hours is determined by the user. Given the differences in capacity and available flexibility with which these events are handled across various power systems, no standard definition for the ramp event has been agreed upon to date [65][66]. Because the power signals for load/net-load are more stable than those for wind/PV, lower threshold values are given to load/net-load ramp events than to wind/PV ramp events. From the perspective view of the network operators, the down-ramps that occurred in the output power of wind/PV are often more difficult to control than up-ramps that could be handled with adjustment to schedules of other generators or, if necessary, by cutting wind/PV production. While the power system operators must adjust for the shortfall of wind/PV when downward ramps take place, by boosting production from the remaining generators available or by inserting additional generators to cover that deficit and maintain a balanced load. So, the threshold value of the ramp-down was chosen smaller than the ramp-up. For PV generation, diurnal up-ramps that are expected from sunrise to midday and expected down-ramps, which are taking place from midday to sundown should not be characterised as ramp events [67].

2.2. Ramp Metrics

The variability analysis can describe wind fluctuations that took place during the studied time to be employed by the grid operators to commit or dispatch the proper generation even in cases of considerable prediction errors [68]. The following metrics will be used in describing the power ramps within 15 minutes time intervals using the historical readings:

a. Ramp characteristic indicators (RCIs)

The electricity systems continuously increase RG's installed capacity, impacting the ramping behaviour of RG. RCIs have been utilized to compare the ramping behaviour of RG in a power system across different years, and they can be used also in comparing the power ramping characteristics in different regions, where the statistical parameters of power ramps over a defined time period Δt are divided by the average installed RG capacity over the year as follows:

$$RCI_{max+/-} = \frac{\Delta p_{max+/-}}{average\ installed\ VRG\ capacity} \qquad (1)$$

$$RCI_{RR} = \frac{Ramping\ Range\ (RR)}{average\ installed\ VRG\ capacity} \qquad (2)$$

$$Ramping\ range = \Delta p_{max+} - \Delta p_{max-} \qquad (3)$$

Where +/↑ refers to the upward ramp, -/↓ refers to the downward ramp, Δp_{max} is the maximum value of ramps over a defined time period, and $RCI_{max,RR}$ is the RCIs for the values of maximum and ramping range (RR). For the average ramp (Δp_{avg}) and standard deviation (σ), the RCIs are calculated as follows:

$$RCI_{avg+/-} = \frac{\Delta p_{avg+/-}}{average\ installed\ VRG\ capacity} \qquad (4)$$

$$RCI_{\sigma+/-} = \frac{\sigma_{+/-}}{average\ installed\ VRG\ capacity} \qquad (5)$$

b. Coefficient of Variation (CV):

It measures the spread of a dataset and compares the variability in the various distributions to illustrate the degree of variability with respect to the mean value [69][70], dividing the standard deviation by the average gives the CV that is calculated for both types of power ramps as follows:

$$CV_{↑↓} = \frac{\sigma_{+/-}}{\Delta p_{avg+/-}} \qquad (6)$$

In the time frame investigated, if the CV value is less than one, the variation is modest and the average value reflects the period's ramps. If the CV value is higher than one, the variation is high and the average in that period does not accurately reflect the power changes. The CV may also be used to compare the variability of various power systems. If the average value is positive, it signifies that throughout the investigated time the upward ramp was more prevalent, whereas a negative value indicates the ramp-down type was more prevalent.

c. Ramp Regularity Factor (RRF):

It is calculated by dividing the average value of ramps over the investigated time period by the maximum of the same type.

$$RRF\ ↑↓= \frac{\Delta p_{avg+/-}}{\Delta p_{max+/-}} \quad , \qquad 0<RRF<1 \qquad (7)$$

When the RRF is near to one, it indicates that the fluctuations are relatively constant as the difference between the average and the maximum values is small, while the values around 0 demonstrate that an unusually high ramp in this period is highly probable since the gap between the average and maximum values is large and the average does not properly reflect the power ramps in this interval. Accordingly, the power system operators should take the required precaution.

d. Ramp Intensity Factor (RIF):

It is used to assess ramp strength by dividing the ramp value (Δp) in an investigated time period by the highest preceding ramp value in that time period with the same direction. The values of RIF that are near 0 reflect minor ramps which may be disregarded, whereas values near 1 represent significant ramps. Hence, it could be used to categorize ramps.

$$RIF = \frac{\Delta p_{+/-}}{\Delta p_{max+/-}} \qquad 0 \leq RIF \leq 1 \qquad (8)$$

The RIF is time-dependent, depending on Δt. when calculating RIF for each observational time t, the degree of ramp strength, in this case, is a function of t and Δt, as the RIF depends on a localized maximum value of preceding ramps at this observational time ($RIF_t \uparrow\downarrow (t, \Delta t)$). Whilst when using the RIF to characterize monthly, seasonal, or yearly ramps over the investigated time period Δt, the degree of ramp strength is measured in regard to a globally maximum value of preceding ramps at this period. The RIF can also be used in measuring the intensity difference of the locally maximum ramp values at each observational time t compared to the globally maximum value that occurred over the same period for each type of ramp. If Δp_{maxt} is the maximum ramp value at an observational time t and $his \; \Delta p_{maxd}$ is the maximum ramp value over a number of days studied, the RIF for locally maximum ramp values (RIF_m) is expressed as follows:

$$RIF_{m\uparrow\downarrow} = \frac{\Delta p_{maxt+/-}}{his \; \Delta p_{maxd+/-}}, \qquad \begin{matrix} 0 \leq RIF_m \\ \leq 1 \end{matrix} \qquad (9)$$

e. Maximum Ramp Ratio (MRR):

The ratio of the maximum values of both types of ramps over the investigated time period, with the maximum downward value divided by the maximum upward value. From the standpoint of grid operators, downward ramps in wind/PV are not easy to control compared to upward ramps, while the upward ramps in load/net-load are not easy to control compared to downward ramps. Hence, the highest ramps values of both types over the investigated time period are compared to obtain the MRR, as follows:

$$MRR = \frac{\Delta p_{max-}}{\Delta p_{max+}} \qquad (10)$$

2.3. Reserve Estimation Methods

The methods for estimating the required reserves differed greatly. The reserve calculation methods can be classified as empirical, deterministic, and probabilistic as follows:

a. Deterministic

The reserve is set so that the system would be capable of withstanding the loss of the largest generating unit, transmission line, or HVDC connections with other interconnected systems. In most power systems, it is calculated based on the largest generating unit (N-1), or even simultaneous loss of some power generating units (N-k).

b. Empirical

The empirical method is used to determine reserve requirements based on historical observations [42]. For example, the so-called 'square root formula' or 'empirical formula' has been used in continental Europe [71][72]. The reserve needs have been calculated depending on operators' expertise and set assumptions based on their practices [73]. Any empirical method is necessarily restricted to variations or events that have happened before. The empirical methods are insensitive to the shares of wind power and can result in higher-risk operational conditions for power systems with a high wind power penetration.

c. Statistical/Probabilistic

The power systems are currently moving toward statistical and probabilistic methods in reserve calculation that are based on the statistical characteristics of events in the power system due to the increase in RG shares. Therefore, both operational practice and integration analysis use the statistical analysis of wind power time series for reserve estimation. [41][56][74]. There is a major gap between the probabilistic approach and the other two methods. The deterministic method has the lowest complexity and data requirements but can ensure mainly security. The latter benefit may come at the disadvantage of an excessive amount of reserves. Finally, the deterministic method is not necessarily appropriate for various emerging risks, including those induced by VRG [75][45], and cannot be scaled to different time horizons. The last limitations refer even to the empirical method that is, by definition, "looking back". The use of empirical approaches often includes the possibility of missing such hazards that exist but have not yet been encountered. Probabilistic methods need more intensive data and computational efforts [76]. Nevertheless, they can deal with multiple and emerging risks, and they are particularly well-suited for stochastic effects such as RG forecast errors and variability. Moreover, they can determine the residual risk level, which permits informed decisions on the balance between security and costs.

2.4. Case Study

Belgium plans to increase rapidly the RG shares for achieving its decarbonization goals, especially from wind generation, instead of nuclear plants, which will be phased out within four years and make up about a third of all installed generating capacity. The decommissioning plan in Figure 1 demonstrates the proposed phase-out time for each nuclear reactor, where the shutdown date for the latter reactor, D2, is set for December 2025 [77]. As a result, wind capacity increased by 154.58% from 1834.71 MW at the end of 2015 to 4,670.83 MW at the end of 2020. In 2020, RG (just wind and solar power) contributed to 18.6% of total electricity generation, up 31% from 2019. The distribution of onshore wind assets in Belgium is presented in Figure 2, the size of the bubbles symbolizes the installed capacity [77][47]. Onshore wind is expected to grow by 120-360 MW per year until 2032, reaching 4.2-6.6 GW. Due to a lack of large open spaces and the need to keep setback distances because of noise pollution from wind turbines, onshore wind turbines are located as illustrated in [78] across more than 150 sites in small groups with 2.4 GW in 2020. As a result, despite their higher cost when compared to onshore wind farms, offshore wind farm construction has increased, making Belgium among the top five countries globally for total offshore wind installations in 2020. 2.262 GW, made up of 394 offshore wind turbines, has already been installed in the North Sea, taking up a total area of 238 km² and having the capacity to meet up to 10% of Belgium's total energy needs. Along with this increase in installed offshore capacity, there has also been an increase in capacity per turbine. Figure 3 shows the current offshore wind installations in the north sea and depicts a new 285 km² region made up of three zones that represent expected offshore wind expansions over the following years, with an additional capacity of 2 GW, hence, the total offshore wind capacity will reach 4.4 GW by 2028 [79][80]. Despite the fact that Belgium did not meet its 13% renewable energy share in energy objective for 2020, data demonstrate that the country is on the correct path and that meeting its 2030 objectives will not be difficult. The COVID-19 pandemic, which forced the government to extend the deadlines for commissioned projects while Belgium went through two rounds of extreme lockdown, may be the cause for not meeting the 2020 objectives [81]. The COVID-19 pandemic may be to blame for the 7% decrease in overall load compared to the preceding five years' average. The electricity consumption throughout the first phase of the lockdown was 25% lower than usual at some periods of the day. [77]. However, there were 119 hours in 2020 when renewable energy provided more than half of the consumed electricity, which has never happened previously. Moreover, nuclear power supplied 39.1% of demand, down from 48.7% in 2019. The majority of this decline was offset by RG [82][47].

Wind speeds at hub heights (above 70 m) for wind turbines typically range between 8.4 and 10.2 m/s on average [83]. The geographic distribution of Belgium's average wind speed is shown in Figure 4. Since the offshore wind speed is higher than that of onshore, the output power of the accompanying generator is also higher [84]. Additionally, the offshore winds do not significantly change with height and are more predictable and consistent than onshore winds, which somewhat reduces the level of wind power intermittency. Onshore wind turbine capacity factors in Belgium in 2019 were 30%, which is nearly half of the offshore wind turbine capacity factors of 53%. The power variations may be increased or decreased depending on the spatial distribution of wind capacity. The time scales and separation between wind farms have an impact on the correlation of wind power output. Longer-term variations in wind power from various sites have a high correlation, and as the correlation increases, the required reserve increases. Short-term variations in wind power from various sites are uncorrelated and random [85][86]. Considerable forecasting errors frequently occur, even with hourly forecasts, and have an impact on reserve needs. In [87], the authors reviewed how capacity adequacy regulations are applied to wind generation in different countries. In Belgium, Loss Of Load Expectation, or LOLE, is used to express the requirements for the goal level of system adequacy, which has been set to 3 h/year and 20 hours once every 20 years [58]. The wind power effect indirectly on the capacity market through adequacy assessment to determine the volume of strategic reserves that is done annually using a probabilistic analysis (Monte Carlo simulation), in which historical wind speeds and hourly dispatch models for various scenarios are used to calculate the volume needed to meet the LOLE target. Strategic reserves are distinct from and in addition to operating reserves. A strategic reserve is a committed volume of capacity that is maintained in reserve outside of the energy-only market. If certain requirements are satisfied, such as a scarcity of supply in the spot market or a price settlement above a particular electricity price, the reserve capacity is only used. In [58], the challenges, the recent statistics, and the future condition of wind and solar energy as the main intermittent RES used in Belgium were reviewed. Three types of reserves exist in Belgium. The primary reserve, known as the Frequency Containment Reserve (FCR), is responsible for maintaining the frequency within the range of 49.8 to 50.2 Hz. Its response time must be less than 30 seconds. The secondary reserve, known as the Automatic Frequency Restoration Reserve (aFRR), is designed to relieve pressure on the FCR by regulating the frequency to 50 Hz. Every ten seconds, all the power plants involved in the aFRR provision receive the set-point signal, which is derived from continuous measurements of the difference between import and export balances. Additionally, tertiary reserve, or manual Frequency Restoration Reserve

(mFRR), is utilized to alleviate the strain on the aFRR reserve, its response time ranging from a few minutes to 15 minutes. mFRR activates when aFRR gets saturated. A variety of sources, including operational generating units, non-operating units with short startup times, and distribution and transmission network customers, can provide the tertiary reserve [58]. However, Belgium's capacity mechanism is now being reviewed.

Applying the ramp metrics discussed above, the variability of the output power recorded every 15 min from 2015 to 2019 of aggregated wind farms (onshore and offshore) in Belgium will be studied. Also, the best fit probability distribution to these short-term variations during this period will be studied, and the multiplier of the standard deviation of these variations will be investigated to estimate the reserve needs that cover these variations within a given degree of certainty.
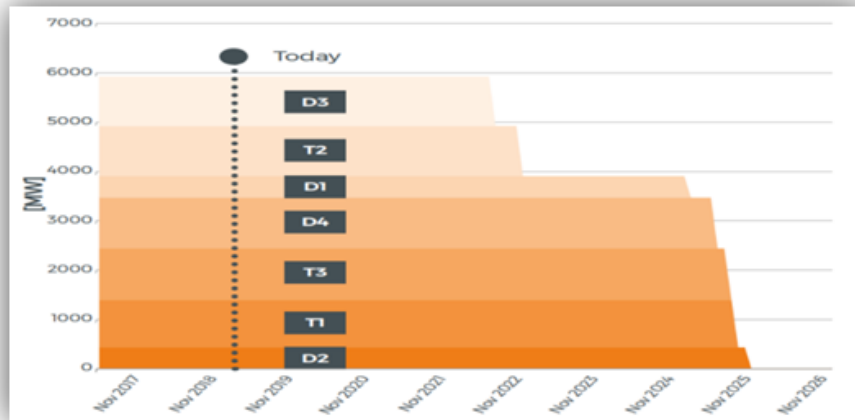
Figure 1. Belgian nuclear plants' phase-out schedule

Figure 2. Geographical distribution of Belgium's installed onshore wind capacity [77][47]
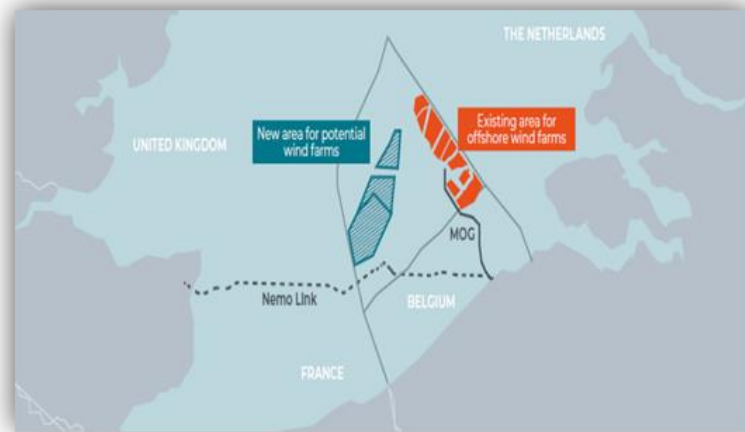
Figure 3. Reserved areas for Belgium's existing and planned offshore wind farms [80]
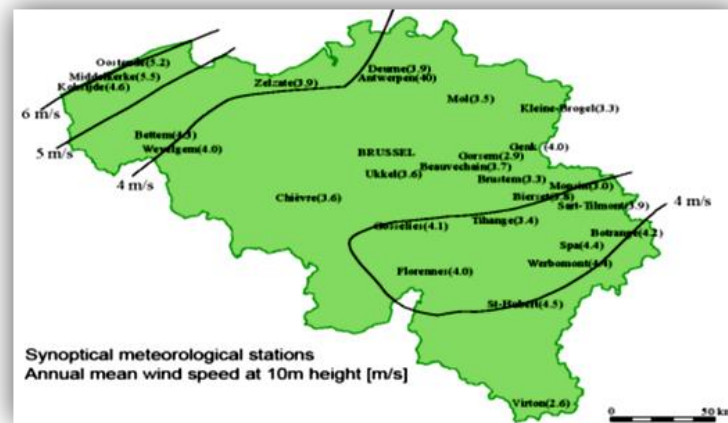
Figure 4. Map of Belgium's annual mean wind speed [88].

3. DATA AVAILABILITY

The datasets analysed during the current study of aggregated wind farms' output power recorded every 15 minutes in Belgium are available in [Wind-power generation (elia.be)] [89].

4. RESULTS AND DISCUSSION

4.1. Analysis of Power Ramps Within 15 Minutes at Each Observational Time *t* Over the Five Years

For the majority of observation times, the values of CV are about equal and greater than one, demonstrating the high variability of the output power within this short-time-interval; thus, it is not correct to rely on the average ramp value at these observation times, as it does not describe correctly the occurred ramps, see Figure 5. The values of CV↑ increase in the late evening and range from 0.88 to 1.85 over the five years, with average values ranging from 1.11 to 1.176, whereas the values of CV↓ range from 0.879 to 2, with average values ranging from 1.107 to 1.182. Hence, the CV values range and their average values for both types of ramps over the five years are about equal and did not change even with the increase in the installed capacity. The RRF↑ percentages across all observation times over the five years range from 4.42% to 25.59%, with average percentages ranging from 13.62 to 14.86%, whereas RRF↓ percentages over the five years range from 3.95% to 25.7%, with average percentages ranging from 13.1 to 14.53%, see Figure 6. Therefore, the RRF values range and their average values for both types of ramps over the five years are about equal. Hence, while the installed capacity increased, the RRF values did not change. The low RRF values near zero indicate that the probability of occurrence of unforeseen high ramps is high, and also illustrate the high wind generation variability within this short-time interval so that the average ramp value does not constitute the actual variation.

Figure 7(a) shows the $RIF_m\uparrow$ values at each observation time over the five years, which vary from 14.1% to 100%, with average percentages ranging from 30.4% to 52.6% and having high values in the late evening and early morning. In Figure 7(b), the $RIF_m\downarrow$ values vary from 14.27% to 100%, with average percentages ranging from 29.67% to 49.28%. The intensity of the local maximum values for the two ramps types varies greatly between times of observation, and this is reflected in the range of RIF_m.

In the most of observation times in Figure 8, the MRR values over the five years seem fairly close to each other, but the range is different. However, the average percentages of MRR over the five years are about equal and greater than 100% (106.5%-119.5%), implying that the downward ramps have higher maximum values than upward ramps to some extent. The results of applying the ramp metrics at all observation times in the five years are summarized in Table 1, demonstrating the range and the average percentage of each metric.

(a)   (b)
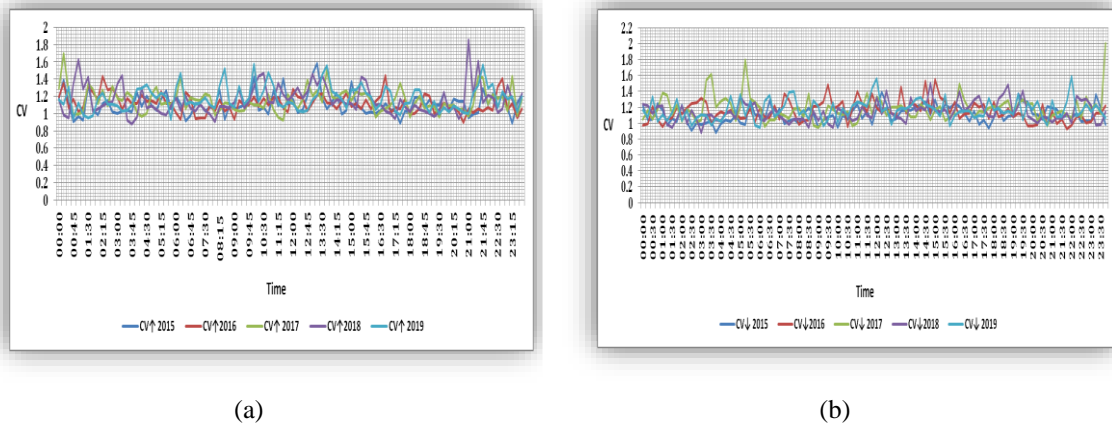
Figure 5. Comparison of CV at each time of observation for each year from 2015 to 2019 (a) CV↑ (b) CV↓

(a)   (b)
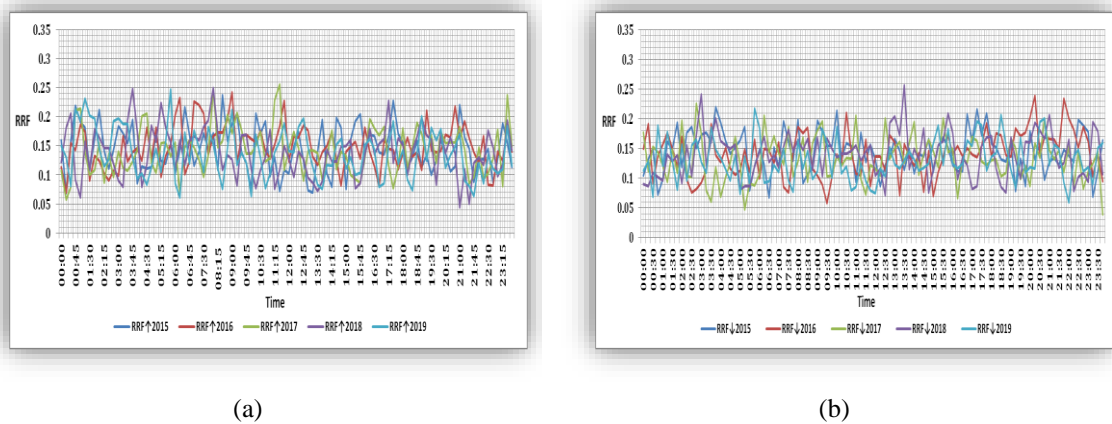
Figure 6. Comparison of RRF at each time of observation for each year from 2015-2019 (a) RRF↑ (b) RRF↓

(a)   (b)
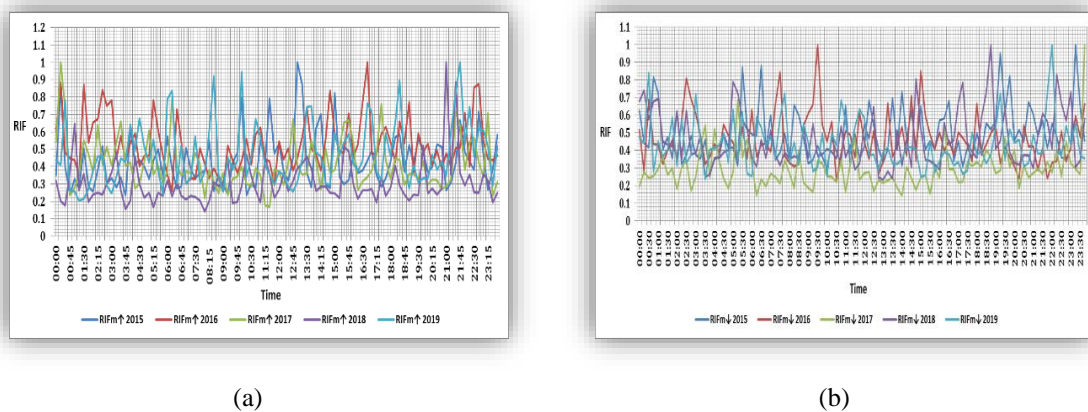
Figure 7. Comparison of RIF_m at each time of observation for each year from 2015-2019 (a) $RIF_m\uparrow$ (b) $RIF_m\downarrow$
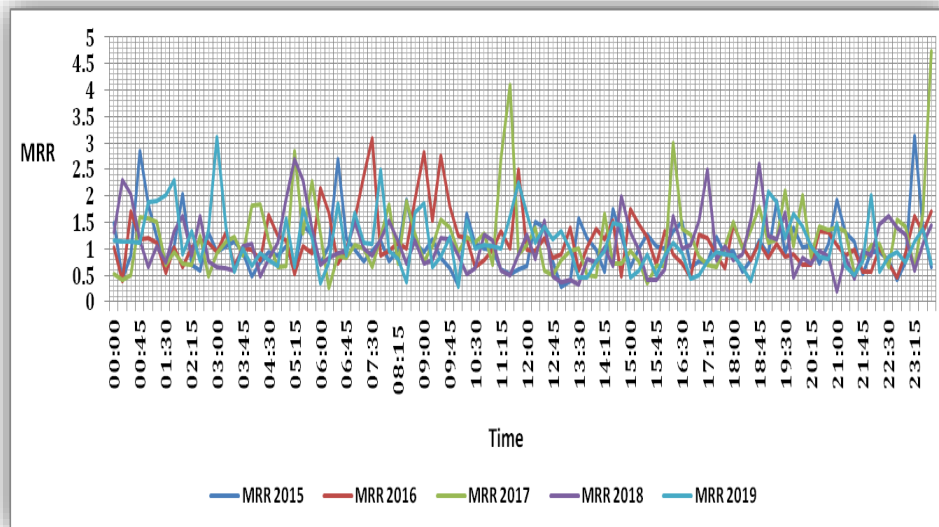
Figure 8. Comparison between MRR values at each time of observation for each year from 2015 to 2019

While the average values and the standard deviations of both types of ramps across all the observation times studied in Figures 9-11 increase as the capacity of the wind installations increases, RCIs for the five years are approximately equal, see Figures 12, 13. Figure 9(a) shows that the average ramp values at all observation times are around zero which confirms the results in [50]. The average ramp values tend to be positive between 10:30 and 22:30, indicating that the upward ramps occur mostly in this period, and tend to be negative in the other periods, indicating that the downward ramps occur mostly in these periods, which shows the changes in output power of wind between up and down ramps throughout the day long. The relative frequency (RF) for each type of ramp in Figure 17 confirms this result. The comparison between the average values and the standard deviations of both types of ramps shows that the standard deviation values are equal to or slightly greater than the average values, demonstrating the high level of variability in wind power within this short period; thus, the average ramp values do not characterize the actual ramps.

The maximum values of both types of ramps and RR increase as the installed wind capacity increases as shown in Figures 14, 16(a), but the corresponding RCIs approximately remain constant, see Figures 15, 16(b). The results reveal that the maximum values of both types of power ramps within 15 minutes can exceed 25% of the capacity of the wind installations.

In Figure 17(a), the numbers of upward ramps over the five years studied are nearly equal across all observation times studied, but increase between 10:30 and 22:30, where the relative ramp-up frequency exceeds 50% during this period. While in Figure.17(b), the total numbers of downward power ramps nearly have the same values in most observation times but their numbers decrease during the period between 10:30 and 22:30, as the relative ramp-down frequency falls below 50% during this period. This reveals that the number of downward power ramps exceeds the number of upward power ramps in the morning, while in the evening, the number of upward power ramps exceeds the number of downward power ramps. This is because wind speeds are lower in the morning and as the temperature rises during the day, wind speeds also rise due to pressure differences and thermal convection. Based on a dataset for just two years, this daily cycle was noticed in the long-term ramps (more than 2h) in [11], whereas there was no clear diurnal pattern in the short-term ramps. A rapid change in the number of power ramps occurred between 3:00 AM and 3:30 AM, from a large number of downward ramps at 3:00 AM to a high number of upward ramps at 3:30 AM, as seen also by the average ramp values shown in Figures 9(a),10, and 12. This rapid change appeared also in [50] at 2:34 AM when short-term fluctuations in the output power of wind farms in Japan were studied. This was due to a steep decline in wind generation when the wind speed surpassed the generator's cutout speed, which is typically set to 25 m/s. While the ranges and average values of the studied ramp variables increase by increasing the capacity of the wind installations, RCIs illustrate that these variables nearly have fixed percentages of the average installed wind capacity and can be estimated in the planning stage when increasing the share of wind generation, see Table 1.
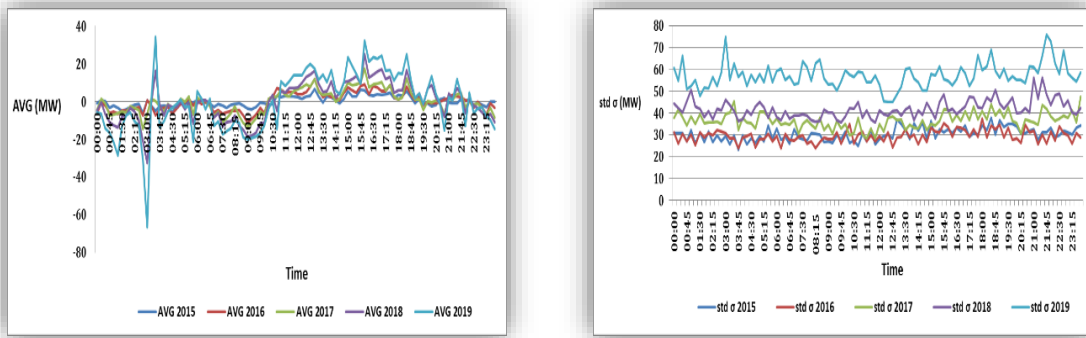
(a)   (b)

Figure 9. Comparison of the average ramp values and the standard deviation of ramps at each time of observation for each year from 2015-2019 (a) Average ramp values (b) The standard deviations
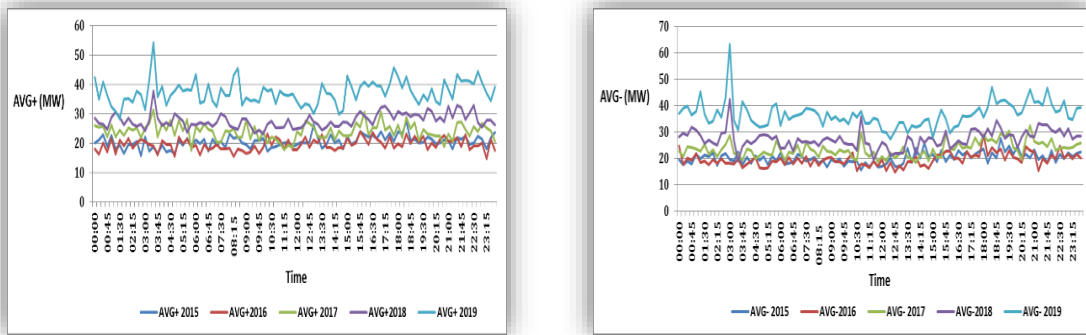
(a)   (b)

Figure 10. Comparison between the average values of both types of ramps at each time of observation for each year from 2015 to 2019 (a) The average values of upward ramps (b) The average values of downward ramps
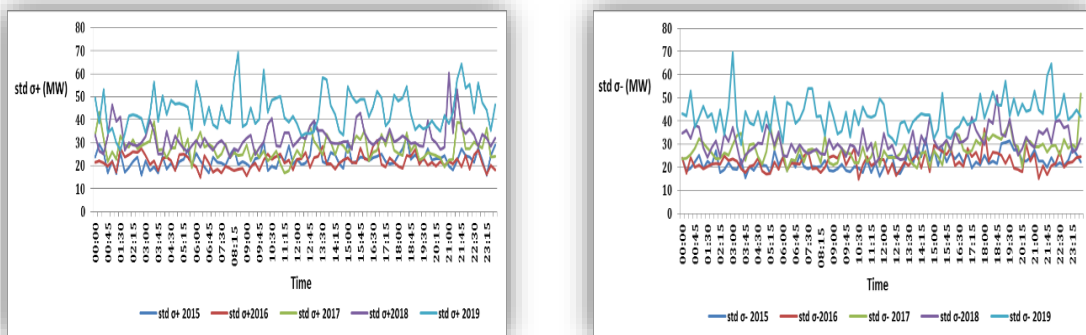
(a)   (b)

Figure 11. (a) The standard deviation of upward ramps (b) The standard deviation of downward ramps

(a)

(b)
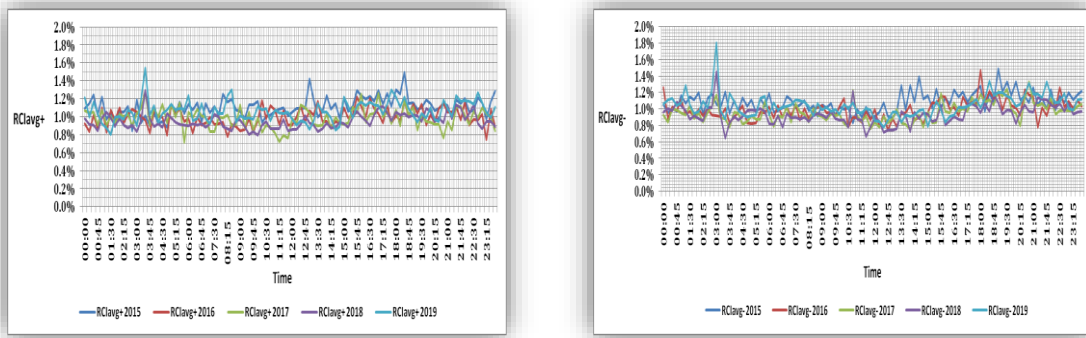
Figure 12. Comparison of RCI$_{avg}$ at each observation time for each year (2015-2019) (a) RCI$_{avg+}$ (b) RCI$_{avg-}$

(a)

(b)
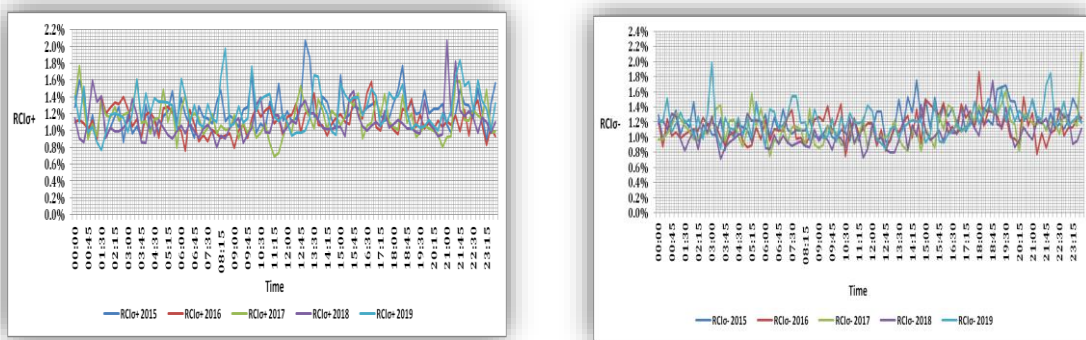
Figure 13. Comparison of RCI$_{\sigma}$ at each time of observation for each year from 2015-2019 (a) RCI$_{\sigma+}$ (b) RCI$_{\sigma-}$

(a)

(b)
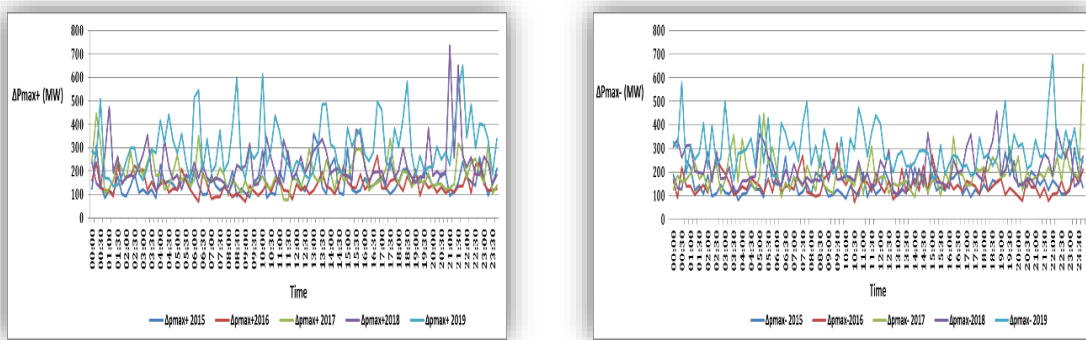
Figure 14. Comparison of the maximum values of ramps at each observational time for each year from 2015 to 2019 (a) The maximum values of upward ramps (b) The maximum values of downward ramps

(a)   (b)
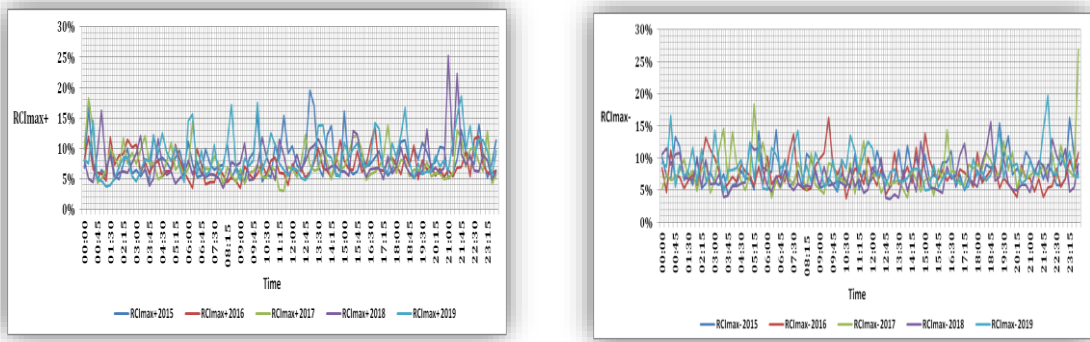
Figure 15. Comparison of RCI_{max} at each time of observation over the five years (a) RCI_{max+} (b) RCI_{max-}

(a)   (b)
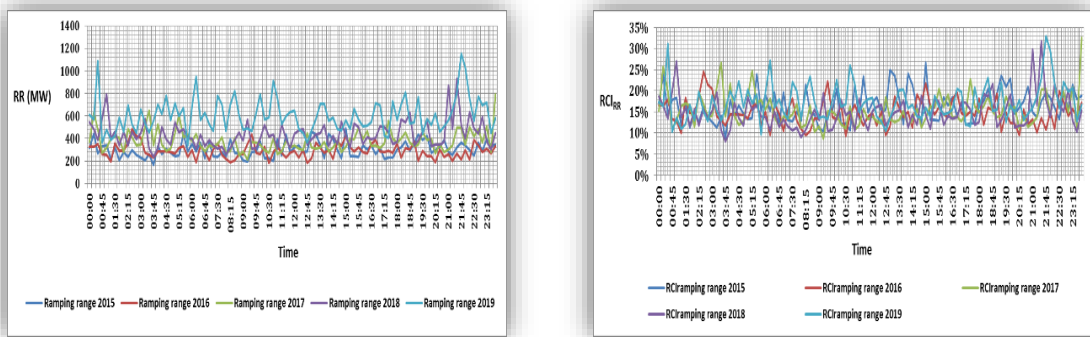
Figure 16. (a) Comparison of the ramping range at each time of observation for each year from 2015 to 2019
(b) Comparison of $RCI_{ramping\ range}$ at each observational time for each year from 2015 to 2019

(a)   (b)
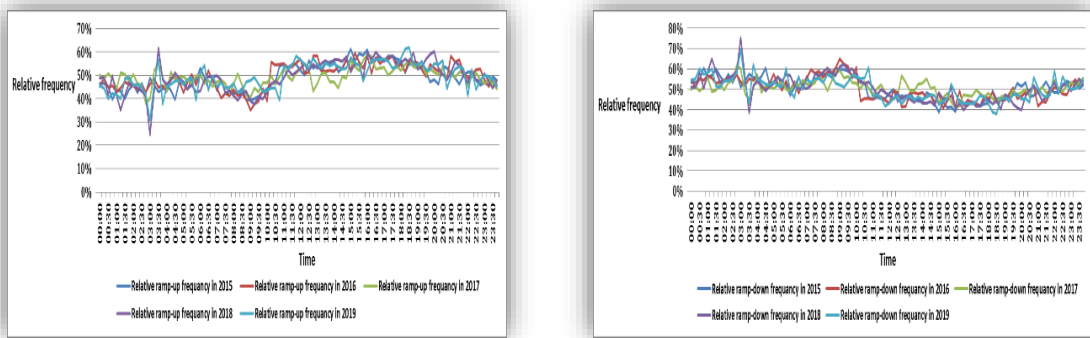
Figure 17. Comparison of the relative frequency of ramps at each observational time for each year from 2015 to 2019 (a) The relative ramp-up frequency (b) The relative ramp-down frequency

Table 1. The range and average percentages of ramp metrics across all times of observation in the five years

Metric	2015 Avg.	Range From	To	2016 Avg.	Range From	To	2017 Avg.	Range From	To	2018 Avg.	Range From	To	2019 Avg.	Range From	To
$RIF_m\uparrow$	43.07	23.39	100	52.68	25.74	100	41.65	16.97	100	30.46	14.1	100	47.06	20.41	100
$RIF_m\downarrow$	49.28	26.45	100	47.14	22.74	100	29.67	14.27	100	46.42	23.38	100	43.49	23.76	100
RCI_{RR}	16.42	8.91	26.65	14.84	9.32	26.72	15.55	8.70	32.52	14.94	8.06	31.80	17.32	9.73	32.89
$RCI_{max}\uparrow$	8.41	4.57	19.52	7.15	3.50	13.58	7.58	3.09	18.21	7.67	3.56	25.22	8.74	3.79	18.57
$RCI_{max}\downarrow$	8.01	4.30	16.25	7.69	3.71	20.39	7.97	3.83	26.85	7.27	3.65	15.60	8.58	4.69	19.74
$RCI_{avg}\uparrow$	1.11	0.85	1.49	0.99	0.75	1.22	0.98	0.72	1.29	0.95	0.79	1.29	1.06	0.81	1.55
$RCI_{avg}\downarrow$	1.09	0.83	1.49	0.99	0.74	1.47	0.96	0.75	1.33	0.93	0.65	1.45	1.04	0.77	1.80
$RCI_\sigma\uparrow$	1.23	0.86	2.07	1.12	0.76	1.58	1.14	0.69	1.77	1.10	0.81	2.07	1.26	0.77	1.97
$RCI_\sigma\downarrow$	1.2	0.83	1.75	1.15	0.74	1.87	1.13	0.75	2.12	1.06	0.71	1.75	1.22	0.85	1.99
$CV\uparrow$	111.1	88.82	158.0	112.2	90.12	144.4	115.4	92.62	169.99	115.7	88.24	185.3	117.6	93.7	157.5
$CV\downarrow$	110.7	87.9	139.3	115.5	93.10	165.3	118.2	94.68	200.4	113.8	88.1	149.8	116.8	94.49	159.1
$RRF\uparrow$	14.48	6.86	23.73	14.86	6.97	24.18	14.22	5.71	25.59	13.87	4.42	24.98	13.62	6.16	24.63
$RRF\downarrow$	14.53	6.82	22.02	14.01	5.51	23.82	13.25	3.95	22.54	13.99	7.09	25.70	13.10	5.89	21.75
MRR	106.5	27.4	313.96	116.7	38.64	322.6	119.5	26.61	473.4	107.2	18.42	270.2	112.2	28.63	312.0

3.2. Monthly Analysis of Power Ramps Over the Five Years

Table 2 shows the range and the average percentages of ramp metrics for both types of ramps within 15 minutes time intervals across all months in the five years, which illustrates that these variables nearly have fixed percentages of the average installed capacity, therefore they can be estimated in the planning stage when increasing the share of wind generation. The results of $CV\uparrow$ for each month in the five years illustrate that all months have approximately equal values except to some extent July 2018. The average percentages of $CV\uparrow$ over the five years are equal and exceed 100% (111.86%-118.58%). The percentage of $CV\uparrow$ across all months over the five is between 91.46% and 176.17%, with all months in 2019 above 100%. Also, the $CV\downarrow$ values over the five years are about equal and their average percentages are equal and more than 100% (110.54%-119.66%). The percentage of $CV\downarrow$ across all months over the five is between 95.51% and 143.77%, with all months in 2016 above 100%. Accordingly, the five years are nearly similar in range and average of CV values for both types of ramps. The CV values of most months are more than one, indicating the high wind variability and the average ramp value in these months can not be used to express the actual ramps.

For both types of ramps, the range and the average values of RRF in the five years are equal. These low percentages of RRF in all months indicate that an unusually high ramp is highly probable since the gap between the average and maximum values is large and the average does not properly reflect the occurred ramps. Accordingly, adequate reserves should be provided for those severe, unexpectedly ramps.

The intensity degree of the highest ramp varies greatly between months, as the percentage of $RIF_m\uparrow$ across all months in the studied years ranges from 26.04% to 100%, with an average percentage between 46.59% and 78.66%, and all the studied years are above 65% except 2018 (46.59%). The $RIF_m\uparrow$ percentage of 100% repeated twice in July and once in March, June, and October. While $RIF_m\downarrow$ percentages range from 34.24% to 100%, with average percentages between 49.84% and 69.83%, and all the studied years are above 63% except 2017 (49.84%). The $RIF_m\downarrow$ percentage of 100% repeated twice in February and once in January, October, and November.

The range and average values of MMR across all months in the five years are roughly equal, with MRR ranging from 45.86% to 207.93%, with an average percentage in the five years between 90.7% and 117.3%. The MRR in July and August is less than 100% over the five years, indicating the maximum downward ramps is less than that of upward ramps. For seasonal analysis, the MRR over the five years is less than 100% in the summer, and the highest values for up and down ramps are quite convergent in the fall.

Compared to other seasons, the RCI_{avg} values of both types of ramps over the five years are high in the fall (their percentages >1%), especially in November. In [50], the maximum ramp values in November were larger than in the other months. The RCI_σ percentages are more than 1% in most months and their percentages are slightly more than that of RCI_{avg} over the five years for both types of ramps, see Table 2.

The $RCI_{max}\uparrow$ percentages across all months in the five years are between 6.57% and 25.22%, with average percentages between 10.51% and 14.01%, while the $RCI_{max}\downarrow$ percentages are between 5.83% and 26.85%, with average percentages between 10.75% and 13.03%. The range and average percentages of both types of RCI_{max} are about equal. The $RCI_{max}\uparrow$ percentages over the five years are not less than 10% in August and all months of 2019 except May. The $RCI_{max}\downarrow$ percentages over the five years are not less than 10% in October and November. The RCI_{RR} percentages over the five years are between 12.4% and 39.76%, with average percentages between 21.27% and 26.32%.

Table 2. The range and average percentage of ramp metrics across all months in the five years

Ramp Metrics	2015			2016			2017			2018			2019		
	Avg.	Range		Avg.	Range		Avg.	Range		Avg.	Range		Avg.	Range	
		From	To		From	To		From	To		From	To		From	To
RCI_{RR}	24.37	18.76	31.86	21.27	17.19	26.91	24.64	17.83	39.76	22.70	12.40	36.79	26.32	19.12	35.09
MRR	95.25	57.24	141.9	103.1	69.52	153.9	117.3	51.42	207.9	103.1	45.86	146.2	90.74	62.60	179.2
Upward Power Ramps															
RCI_{max}	12.79	9.18	19.52	10.51	8.53	13.58	11.61	7.00	18.21	11.86	6.57	25.22	14.01	9.25	18.57
RCI_{avg}	1.11	0.90	1.41	1.00	0.81	1.28	0.98	0.75	1.31	0.95	0.73	1.13	1.07	0.87	1.40
RCI_{σ}	1.24	1.04	1.59	1.12	0.91	1.32	1.14	0.89	1.51	1.10	0.72	1.35	1.26	0.98	1.57
CV	111.9	91.46	128.4	112.6	97.60	125.7	116.4	94.26	139.7	116.4	97.32	176.2	118.6	105.9	136.7
RRF	9.21	5.93	13.17	9.61	7.32	13.31	8.99	6.14	13.68	9.53	2.91	15.31	7.83	5.48	10.62
RIF_m	65.64	47.04	100.0	78.66	62.84	100.0	65.15	38.47	100.0	46.59	26.04	100.0	74.68	49.81	100.0
Downward Power Ramps															
RCI_{max}	11.58	7.85	16.25	10.75	7.36	16.31	13.03	9.19	26.85	10.84	5.83	15.60	12.31	7.36	19.74
RCI_{avg}	1.09	0.87	1.41	0.99	0.77	1.29	0.96	0.73	1.28	0.94	0.68	1.12	1.05	0.88	1.38
RCI_{σ}	1.20	1.01	1.65	1.13	0.85	1.42	1.13	0.89	1.44	1.05	0.74	1.31	1.22	0.91	1.57
CV	110.5	95.51	121.5	114.1	99.56	129.1	119.7	99.27	143.8	113.4	99.06	142.4	116.9	99.37	134.8
RRF	9.70	6.10	14.08	9.54	6.10	13.86	7.94	3.34	12.18	9.07	5.86	12.88	8.99	5.30	12.38
RIF_m	69.83	48.31	100.0	67.08	45.12	100.0	49.84	34.24	100.0	66.68	37.36	100.0	63.22	37.29	100.0

3.3. Yearly Analysis of Power Ramps Over the Five Years

Although the installed wind capacity over the five years is nearly doubled, comparing ramp metrics percentages in 2015 and 2019 reveals that they have very close percentages for all ramp metrics except the MRR, see Table 3. The values of RIF_m are presented in Table 3 as a multiplier of the standard deviation ($\lambda\sigma$), as the yearly value of RIF_m is one. For upward ramps, the values of λ range from 11.09 to 21.66, while they range from 12.49 to 22.51 for downward ramps. These nearly fixed percentages of ramp metrics over the five years aid in dealing with wind variability and uncertainty in power system operation and planning. The results also demonstrate that the maximum power ramp during this short time interval may exceed 25% of the average capacity of wind installations although the percentages of the average power ramps are about 1%, this appears clearly in the percentages of RRF which are less than 8%. The percentages of CV over the five years exceed 100%, demonstrating the high variability of power during this short period.

Table 3. The yearly results of ramp metrics over the five years

Ramp Metrics	2015	2016	2017	2018	2019	Average
RCI_{RR}	35.77%	29.89%	45.05%	40.82%	38.30%	37.97%
MRR	83.25%	120.08%	147.47%	61.86%	106.32%	103.80%
			Upward Power Ramps			
RCI_{max}	19.52%	13.58%	18.21%	25.22%	18.57%	19.02%
RCI_{avg}	1.11%	1.00%	0.99%	0.95%	1.07%	1.02%
RCI_{σ}	1.26%	1.13%	1.16%	1.12%	1.28%	1.19%
CV	113.22%	113.49%	117.67%	117.40%	120.14%	116.38%
RRF	5.70%	7.36%	5.41%	3.78%	5.74%	5.60%
$RIF_m (\lambda\,\sigma)$	14.6 σ	11.09 σ	14.85 σ	21.66 σ	13.66 σ	15.17 σ
			Downward Power Ramps			
RCI_{max}	16.25%	16.31%	26.85%	15.60%	19.74%	18.95%
RCI_{avg}	1.08%	0.99%	0.96%	0.94%	1.05%	1.00%
RCI_{σ}	1.21%	1.15%	1.15%	1.08%	1.25%	1.17%
CV	112.08%	116.68%	120.34%	114.82%	118.62%	116.51%
RRF	6.67%	6.06%	3.56%	6.01%	5.32%	5.52%
$RIF_m (\lambda\,\sigma)$	12.49 σ	13.28 σ	22.51 σ	13.63 σ	14.99 σ	15.38 σ

3.4. Fitting PDF For Short-Term Wind Variations

The goodness of fit tests examines how well each distribution function matches the data. The results assist to select the best model for the data. EasyFit 5.5 software is a data analysis tool that contains a large number of different distribution types (over 60), which enables selecting the probability distribution that best matches the data. The following goodness of fit tests are supported by the program: Kolmogorov-Smirnov, Anderson-Darling, and Chi-Squared. Table 4 presents the results of the goodness of fit tests for the best-fitted probability distributions to variations of wind power within 15 minutes for each year from 2015 to 2019, while Table 5 shows the results of fitting these variations by the normal distribution. The results illustrate that the best-fitted PDFs to wind variations are Laplace PDF and Error PDF, whereas the rank of fitting the wind variations by a normal distribution varies from 9 to 15 over the five years and according to these tests, fitting these variations by a normal distribution is rejected.

Table 4. The results of the goodness of fit tests for the best-fitted probability distributions to variations of wind power within 15 minutes from 2015 to 2019

Year	Best fit PDF	Parameters	Goodness of fitting					
			Kolmogorov-Smirnov		Anderson-Darling		Chi-Squared	
			Statistic	Rank	Statistic	Rank	Statistic	Rank
2015	Laplace	☐=0.01064 ☐=0.08953	0.01006	1	0.43034	1	11.481	1
	Error	k=1.0528 ☐=132.95 ☐=0.08953	0.01454	2	1.2298	2	22.878	2
2016	Laplace	☐=0.01108 ☐=-0.20296	0.01529	1	1.3971	1	19.694	2
	Error	k=1.0 ☐=127.66 ☐=-0.20296	0.01529	2	1.3971	2	19.694	1
2017	Laplace	☐=0.0092 ☐=0.33484	0.02699	1	3.3532	1	45.681	1
	Error	k=1.0 ☐=153.65 ☐=0.33484	0.02699	2	3.3532	2	45.681	2
2018	Laplace	☐=0.00763 ☐=-0.25495	0.02384	1	2.7586	1	22.162	2
	Error	k=1.0 ☐=185.46 ☐=-0.25495	0.02384	2	2.7586	2	22.162	1
2019	Laplace	☐=0.00581 ☐=6.1644E-5	0.0203	1	2.4569	1	26.105	2
	Error	k=1.0 ☐=243.26 ☐=6.1644E-5	0.0203	2	2.4569	2	26.105	1

Table 5. The results of the goodness of fit tests for fitting the normal distribution to variations of wind power within 15 minutes from 2015 to 2019

Year	Parameters of normal distribution	Goodness of fitting								
		Kolmogorov-Smirnov			Anderson-Darling			Chi-Squared		
		Statistic	Rank	Result	Statistic	Rank	Result	Statistic	Rank	Result
2015	☐=132.95 ☐=0.08953	0.0685	11	Reject	47.738	11	Reject	446.71	11	Reject
2016	☐=127.66 ☐=-0.20296	0.07422	12	Reject	57.724	10	Reject	538.13	9	Reject
2017	☐=153.65 ☐=0.33484	0.08053	15	Reject	62.511	13	Reject	664.75	15	Reject
2018	☐=185.46 ☐=-0.25495	0.08284	14	Reject	60.198	12	Reject	565.45	15	Reject
2019	☐=243.26 ☐=6.1644E-5	0.07655	9	Reject	62.46	12	Reject	596.44	11	Reject

The reserve required to cover these short-term variations within a given degree of certainty over the five years is measured as a multiplier of the standard deviation of these variations. Table 6 presents the multiplier of standard deviation for different confidence levels over the five years and also presents these confidence levels as a percentage of average installed wind capacity. As shown in Table 6, the 3σ rule does not cover 99.7% of the short-term variations, and it just covers from 98.19%-98.38%, confirming the results obtained by rejecting the coverage of short-term wind variations by the normal distribution. The multiplier of standard deviation for achieving a confidence level of 99.7% over the five years is between "4.71-5.11". While for achieving a confidence level of 99.9%, it is between "6.12-6.72". If the confidence level decreases to 99%, the multiplier is between "3.46-3.68". The standard deviation of these variations as a percentage of average capacity of the wind installations over the five years is between "1.45-1.65%". Historical patterns of measured output power from wind farms are used to estimate reserves. Accordingly, the multiplier of standard deviation for each confidence level over the five years is within a very narrow band and also the standard deviation of short–term variation as a percentage of the average capacity of wind installations. As a result, the amount of operational reserve caused by wind can be calculated as a function of the capacity of wind installations using the average value of the multiplier over the five years ($\lambda_{\text{avg 5y}}$) for each confidence level. Therefore, the required reserve for short-term wind variation at different confidence levels can be estimated in 2020 as follows:

$$Required\ reserve = \lambda_{\text{avg 5y}} * \sigma \qquad (11)$$

$$\sigma = C * \text{average installed capacity} \qquad (12)$$

$$Required\ reserve = \lambda_{\text{avg 5y}} * C * \text{average installed capacity} \qquad (13)$$

Where C represents the average standard deviation percentage over the five years. Comparing the estimated reserve in 2020 with that calculated, as shown in Table 7, illustrates that the percentage error at different confidence levels is less than 10% (5.3%-9.2%).
Figure 18 depicts the nonlinear relationship between the required reserve at various confidence levels and the installed wind capacity, and it also demonstrates that the required reserve increases as the capacity of wind installations increases.

Table 6. The standard deviation of short-term wind variations as a reserve measure

year	2015	2016	2017	2018	2019
Average installed capacity (MW)	1849.58	1960.91	2439.07	2922.09	3506.33
σ	30.597 (1.65%)	29.717 (1.52%)	36.78 (1.51%)	42.345 (1.45%)	57.79 (1.65%)
3σ	98.38% (4.96%)	98.19% (4.55%)	98.27% (4.52%)	98.37% (4.35%)	98.28% (4.94%)
99%	3.47σ (5.74%)	3.68σ (5.58%)	3.518σ (5.31%)	3.465σ (5.02%)	3.582σ (5.9%)
99.7%	4.719σ (7.81%)	5.09σ (7.71%)	4.94σ (7.45%)	4.768σ (6.91%)	5.11σ (8.42%)
99.99%	6.12 σ (10.12%)	6.195σ (9.39%)	6.21σ (9.36%)	6.544 (9.48%)	6.724σ (11.08%)

Table 7. Estimation of the required reserve at different confidence levels for short-term wind variations by using the standard deviation as a reserve measure

Standard deviation and Confidence levels	Average from 2015-2019	2020		Error%
		Estimation (MW)	Calculation (MW)	
σ	1.556%	63.133	65.01	2.89%
3σ	4.668%	189.4	195.04	2.89%
99%	3.543σ	223.68	236.23	5.3%
99.7%	4.9254σ	310.955	332.65	6.5%
99.99%	6.3586σ	401.44	442.23	9.2%
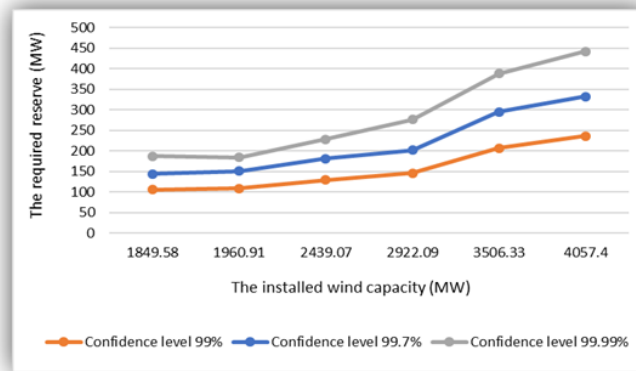
Figure 18. The relation between the required reserve at different confidence levels and the installed wind capacity

5. CONCLUSION

The increasing shares of wind generation have led to more variations and ramp events in netload, thus acquiring more information about such variations is necessary for the power system operators. The linkage between ramp events and meteorological phenomena is highly dependent on the studied case, in addition, a large proportion of these events has not yet been linked to meteorological phenomena.

The actual output power variability of aggregated wind farms in a short period (15 minutes) has been studied over five years from 2015 to 2019 using ramp metrics, which demonstrated that the output power over the five years nearly has similar ramping behaviour, although the share of wind generation is nearly doubled. Therefore, the ramping behaviour can be estimated in the planning stage when increasing the share of wind generation, as these nearly fixed percentages of ramp metrics can facilitate dealing with wind variability and uncertainty in power system operation and planning. The results reveal that the highest values of both types of ramps within 15 minutes can exceed 25% of the capacity of wind installations although the percentage of the average power ramps is about 1%. The seasonal analysis demonstrated that the maximum ramp ratio (MRR) over the five years is less than 100% in the summer, indicating the maximum value of downward ramps is less than that of upward ramps, whereas the highest values for both ramp types are relatively convergent in the fall. For both types of ramps, the values of the ramp characteristic indicator for the average value (RCI_{avg}) over the five years are high in the fall, especially in November. The comparison of the average values and the standard deviation of both ramp types has shown that the standard deviation values are equal to or slightly greater than the average values, so the percentages of coefficient of variation (CV) over the five years exceed 100%, demonstrating the high variability in wind power within this short period; thus, the average values do not describe the real ramps.

The probability distribution of short-term wind power variations that are observed in current system operation is important for modelling the variations that can be expected in future scenarios. For modelling these variations, the various shapes of probability distributions have been examined. The results illustrate that the

best-fitted PDFs to wind variations are Laplace PDF and Error PDF, whereas the rank of fitting the wind variations by a normal distribution varies from 9 to 15 over the five years and according to the goodness of fit tests, fitting these variations by a normal distribution is rejected. The multiplier of the standard deviation of short-term variations is used for measuring the required reserve for these variations. The results demonstrated that the 3σ rule does not cover 99.7% of the short-term variations, and it just covers 98.19%-98.38%, confirming the results obtained by rejecting the coverage of short-term wind variations by the normal distribution that has resulted in a reserve underestimation at a given confidence level. The multiplier of standard deviation for achieving a confidence level of 99.7% over the five years is between "4.71-5.11". While for achieving a confidence level of 99.9%, it is between "6.12-6.72". If the confidence level decreases to 99%, the multiplier is between "3.46-3.68". The standard deviation of these variations as a percentage of average capacity of the wind installations over the five years is between "1.45-1.65%". Therefore, the multiplier of standard deviation for each confidence level over the five years is within a very narrow band and also, the standard deviation of short–term variations as a percentage of the average capacity of wind installations. Using the average value of the multiplier over the five years ($\lambda_{avg\ 5y}$) for each confidence level, the required reserve for short-term wind variations at different confidence levels has been estimated. Comparing the estimated reserve with that calculated has illustrated that the percentage of error at different confidence levels is less than 10% (5.3%-9.2%). The paper also illustrated that the required reserve at various confidence levels increases nonlinearly as the capacity of wind installations increases. Finally, this method is based on high-resolution historical data being available and the data should be updated on a regular basis with increasing wind penetration level, e.g. once a year, to capture the stochastic characteristics of recently measured wind power and to incorporate any smoothing effects. This also means that wind generation was already operational at the time of the study. Time series with a relevant resolution of up to 10-15 minutes are necessary to study short-term variations in wind generation.

REFERENCES

[1]   C. D. Yue, C. C. Liu, C. C. Tu, and T. H. Lin, "Prediction of power generation by offshore wind farms using multiple data sources," *Energies*, vol. 12, no. 4, pp. 1–24, 2019, doi: 10.3390/en12040700.

[2]   H. Díaz and C. Guedes Soares, "Review of the current status, technology and future trends of offshore wind farms," *Ocean Eng.*, vol. 209, no. April, p. 107381, 2020, doi: 10.1016/j.oceaneng.2020.107381.

[3]   International Renewable Energy Agency, "IRENA's renewable energy statistics," 2020. [Online]. Available: https://www.irena.org/publications/2021/March/Renewable-Capacity-Statistics-2021.

[4]   J. Lee and F. Zhao, "Global Wind Report 2021," 2021. [Online]. Available: http://www.gwec.net/global-figures/wind-energy-global-status/.

[5]   IRENA, "Post-COVID recovery: An agenda for resilience, development and equality," 2020. [Online]. Available: /publications/2020/Jun/Post-COVID-Recovery.

[6]   W. P. J. Philippe, S. Zhang, S. Eftekharnejad, P. K. Ghosh, and P. K. Varshney, "Mixed Copula-Based Uncertainty Modeling of Hourly Wind Farm Production for Power System Operational Planning Studies," *IEEE Access*, vol. 8, pp. 138569–138583, 2020, doi: 10.1109/ACCESS.2020.3012437.

[7]   M. S. Eltohamy, M. S. A. Moteleb, H. E. A. Talaat, S. F. Mekhamer, and W. A. Omran, "Overview of Power System Flexibility Options with Increasing Variable Renewable Generations," in *6th International Conference on Advanced Control Circuits and Systems (ACCS) & 2019 5th International Conference on New Paradigms in Electronics & Information Technology (PEIT)*, 2019, pp. 280–292, doi: DOI: 10.1109/ACCS-PEIT48329.2019.9062836.

[8]   G. Limpens and H. Jeanmart, "Quantification of electricity storage needs for Belgium energy transition: A sensitivity analysis based on EROI," *ECOS 2018 - Proc. 31st Int. Conf. Effic. Cost, Optim. Simul. Environ. Impact Energy Syst.*, no. June, 2018.

[9]   M. Koivisto, K. Plakas, E. R. Hurtado Ellmann, N. Davis, and P. Sørensen, "Application of microscale wind and detailed wind power plant data in large-scale wind generation simulations," *Electr. Power Syst. Res.*, vol. 190, no. April 2020, p. 106638, 2021, doi: 10.1016/j.epsr.2020.106638.

[10] G. Ren, J. Liu, J. Wan, Y. Guo, and D. Yu, "Overview of wind power intermittency : Impacts, measurements, and mitigation solutions," *Appl. Energy*, vol. 204, pp. 47–65, 2017, doi: 10.1016/j.apenergy.2017.06.098.

[11] B. R. Cheneka, S. J. Watson, and S. Basu, "A simple methodology to detect and quantify wind power ramps," *Wind Energy Sci.*, no. April, pp. 1–12, 2020, doi: 10.5194/wes-2020-64.

[12] M. Anvari *et al.*, "Short term fluctuations of wind and solar power systems," *New J. Phys.*, no. 18, 2016, doi: 10.1088/1367-2630/18/6/063027.

[13] A. Upadhyay, B. Hu, J. Li, and L. Wu, "A chance-constrained wind range quantification approach to robust SCUC by determining dynamic uncertainty intervals," *CSEE J. Power Energy Syst.*, vol. 2, no. 1, pp. 54–64, 2016, doi: 10.17775/cseejpes.2016.00009.

[14] G. Ren, J. Liu, J. Wan, F. Li, Y. Guo, and D. Yu, "The analysis of turbulence intensity based on wind speed data in onshore wind farms," *Renew. Energy*, vol. 123, pp. 756–766, 2018, doi: 10.1016/j.renene.2018.02.080.

[15] H. Valizadeh Haghi and S. Lotfifard, "Spatiotemporal modeling of wind generation for optimal energy storage sizing," *IEEE Trans. Sustain. Energy*, vol. 6, no. 1, pp. 113–121, 2015, doi: 10.1109/TSTE.2014.2360702.

[16] M. S. Eltohamy, M. S. A. Moteleb, H. E. A. Talaat, S. F. Mekhamer, and W. A. Omran, "Analyzing Wind Power Ramps for High Penetration of Variable Renewable Generation," in *2019 21st International Middle East Power Systems Conference (MEPCON), Cairo, Egypt.*, 2019, pp. 768–775, doi: 10.1109/MEPCON47431.2019.9007951.

[17] M. S. Eltohamy, M. S. A. Moteleb, H. E. A. Talaat, S. F. Mekhamer, and W. A. Omran, "Wind Power Ramps Analysis for High Shares of Variable Renewable Generation in Power Systems," *Indones. J. Electr. Eng. Informatics*, vol. 8, no. 2, pp. 256–272, 2020, doi: 10.11591/ijeei.v8i2.1984.

[18] M. S. Eltohamy, M. S. A. Moteleb, H. E. A. Talaat, S. F. Mekhamer, and W. A. Omran, "Power System Flexibility Metrics Evaluation and Power Ramping Analysis for High Variable Renewable Generation Shares," *EAI Endorsed Trans. Energy Web*, vol. 8, no. 31, pp. 1–23, 2020, doi: 10.4108/eai.13-7-2018.165282.

[19] M. S. Eltohamy, M. S. A. Moteleb, H. E. A. Talaat, S. F. Mekhamer, and W. Omran, "A Novel Approach for the Power Ramping Metrics," *Indones. J. Electr. Eng. Informatics*, vol. 9, no. 2, pp. 313–333, 2021, doi: 10.52549/.v9i2.2612.

[20] N. Pearre, K. Adye, and L. Swan, "Proportioning wind, solar, and in-stream tidal electricity generating capacity to co-optimize multiple grid integration metrics," *Appl. Energy*, vol. 242, no. March, pp. 69–77, 2019, doi: 10.1016/j.apenergy.2019.03.073.

[21] S. Han *et al.*, "Quantitative evaluation method for the complementarity of wind-solar-hydro power and optimization of wind-solar ratio," *Appl. Energy*, vol. 236, no. November 2018, pp. 973–984, 2019, doi: 10.1016/j.apenergy.2018.12.059.

[22] J. P. Deane, G. Drayton, and B. P. Ó. Gallachóir, "The impact of sub-hourly modelling in power systems with significant levels of renewable generation q," *Appl. Energy*, vol. 113, pp. 152–158, 2014, doi: 10.1016/j.apenergy.2013.07.027.

[23] J. Kiviluoma, H. Holttinen, D. Weir, R. Scharff, and L. Söder, "Variability in large-scale wind power generation," *Wind Energy*, vol. 18, no. 11, pp. 1649–1665, 2015, doi: 10.1002/we.

[24] G. Ren, J. Wan, J. Liu, D. Yu, and L. Söder, "Analysis of wind power intermittency based on historical wind power data," *Energy*, vol. 150, pp. 482–492, 2018, doi: 10.1016/j.energy.2018.02.142.

[25] A. J. Deppe, W. A. Gallus, and E. S. Takle, "A WRF Ensemble for Improved Wind Speed Forecasts at Turbine Height," *Weather Forecast.*, vol. 28, pp. 212–228, 2013, doi: 10.1175/WAF-D-11-00112.1.

[26] B. Huang, I. S. Member, V. Krishnan, I. Member, B. Hodge, and I. S. Member, "Analyzing the Impacts of Variable Renewable Resources on California Net-Load Ramp Events," no. August, pp. 1–5, 2018.

[27] F. Zhang, Y. Qiao, and Z. Lu, "Extreme wind power forecast error analysis considering its application in day-ahead reserve capacity planning," *IET Renew. Power Gener.*, vol. 12, no. 16, pp. 1923–1930, 2018, doi: 10.1049/iet-rpg.2018.5023.

[28] W. Dong and S. Li, "Reliability sensitivity of wind power system considering correlation of forecast errors based on multivariate NSTPNT method," *Prot. Control Mod. Power Syst.*, vol. 6, no. 1, 2021, doi: 10.1186/s41601-021-00192-0.

[29] A. A. Thatte and L. Xie, "A metric and market construct of inter-temporal flexibility in time-coupled economic dispatch," *IEEE Trans. Power Syst.*, vol. 31, no. 5, pp. 3437–3446, 2016, doi: 10.1109/TPWRS.2015.2495118.

[30] A. Jonaitis *et al.*, "Challenges of integrating wind power plants into the electric power system : Lithuanian case," *Renew. Sustain. Energy Rev.*, vol. 94, no. June, pp. 468–475, 2018, doi: 10.1016/j.rser.2018.06.032.

[31] S. Goodarzi, H. N. Perera, and D. Bunn, "The impact of renewable energy forecast errors on imbalance volumes and electricity spot prices," *Energy Policy*, vol. 134, no. October 2018, p. 110827, 2019, doi: 10.1016/j.enpol.2019.06.035.

[32] L. Han, H. Jing, R. Zhang, and Z. Gao, "Wind power forecast based on improved Long Short Term Memory network," *Energy*, vol. 189, no. xxxx, p. 116300, 2019, doi: 10.1016/j.energy.2019.116300.

[33] C. Otero-Casal, P. Patlakas, M. A. Prosper, G. Galanis, and G. Miguez-Macho, "Development of a High-Resolution Wind Forecast System Based on the WRF Model and a Hybrid," *Energies*, vol. 12, no. 3050, pp. 1–19, 2019, doi: 10.3390/en12163050.

[34] I. Würth *et al.*, "Minute-scale forecasting of wind power—results from the collaborative workshop of IEA Wind task 32 and 36," *Energies*, vol. 12, no. 4, 2019, doi: 10.3390/en12040712.

[35] S. J. Wellby and N. A. Engerer, "Categorizing the meteorological origins of critical ramp events in collective photovoltaic array output," *J. Appl. Meteorol. Climatol.*, vol. 55, no. 6, pp. 1323–1344, 2016, doi: 10.1175/JAMC-D-15-0107.1.

[36] L. Y. Musilek P, "Forecasting of wind ramp events—analysis of cold front detection."

[37] C. Gallego-Castillo, A. Cuerva-Tejero, and O. Lopez-Garcia, "A review on the recent history of wind power ramp forecasting," *Renew. Sustain. Energy Rev.*, vol. 52, pp. 1148–1157, 2015, doi: 10.1016/j.rser.2015.07.154.

[38] M. Sherry and D. Rival, "Meteorological phenomena associated with wind-power ramps downwind of mountainous terrain," *J. Renew. Sustain. Energy*, vol. 033101, no. 7, pp. 1–13, 2015, doi: 10.1063/1.4919021.

[39] S. Watson, "Quantifying the variability of wind energy," *WIREs Energy Environ.*, vol. 3, pp. 330–342, 2014, doi: 10.1002/wene.95.

[40] H. Huang, M. Zhou, and G. Li, "An Endogenous Approach to Quantifying the Wind Power Reserve," *IEEE Trans. Power Syst.*, vol. 35, no. 3, pp. 2431–2442, 2020, doi: 10.1109/TPWRS.2019.2954844.

[41] C. Rahmann, A. Heinemann, and R. Torres, "Quantifying operating reserves with wind power : towards probabilistic – dynamic approaches," vol. 10, pp. 366–373, 2016, doi: 10.1049/iet-gtd.2015.0538.

[42] D.-C. Radu, "Strategies for Provision of Secondary Reserve Capacity to Balance Short-Term Fluctuations of Variable Renewable Energy," KTH School of Industrial Engineering and Management, 2017.

[43] S. M. M. Agah and D. Flynn, "Impact of modelling non-normality and stochastic dependence of variables on operating reserve determination of power systems with high penetration of wind power," *Electr. Power Energy Syst.*, vol. 97, no. November 2016, pp. 146–154, 2018, doi: 10.1016/j.ijepes.2017.11.002.

[44] S. Collins *et al.*, "Integrating short term variations of the power system into integrated energy system models : A methodological review," *Renew. Sustain. Energy Rev.*, vol. 76, no. July 2016, pp. 839–856, 2017, doi: 10.1016/j.rser.2017.03.090.

[45] Elia group, "Methodology for the dimensioning of the aFRR needs," 2020.

[46] M. S. Eltohamy, H. E. A. Talaat, M. S. A. Moteleb, S. F. Mekhamer, and W. A. Omran, "A Probabilistic Methodology for Estimating Reserve Requirement and Optimizing its Components in Systems with High Wind Penetration," *IEEE Access*, pp. 1–21, 2022, doi: 10.1109/ACCESS.2022.3211305.

[47] S. Asiaban *et al.*, "Wind and Solar Intermittency and the Associated Integration Challenges : A Comprehensive Review Including the Status in the Belgian Power System," *Energies*, vol. 14, no. 9, pp. 1–41, 2021, doi: 10.3390/en14092630.

[48] K. De Vos, J. Morbee, J. Driesen, and R. Belmans, "Impact of wind power on sizing and allocation of reserve requirements," *IET Renew. Power Gener.*, no. October 2012, pp. 1–9, 2013, doi: 10.1049/iet-rpg.2012.0085.

[49] H. Holttinen *et al.*, "Methodologies to Determine Operating Reserves due to Increased Wind Power," *IEEE Trans. Sustain. Energy*, vol. 3, no. 4, 2013.

[50] T. Ikegami, C. T. Urabe, T. Saitou, and K. Ogimoto, "Numerical definitions of wind power output fluctuations for power system operations," *Renew. Energy*, vol. 115, pp. 6–15, 2018, doi: 10.1016/j.renene.2017.08.009.

[51] I. Side *et al.*, "Reserve requirements of wind power IEA WIND Task 25 Operating Reserves different in all systems – General definition," 2011.

[52] M. A. Matos and R. J. Bessa, "Setting the Operating Reserve Using Probabilistic Wind Power Forecasts," *IEEE Trans. POWER Syst.*, vol. 26, no. 2, pp. 594–603, 2011.

[53] M. Black and G. Strbac, "Value of bulk energy storage for managing wind power fluctuations," *IEEE Trans. Energy Convers.*, vol. 22, no. 1, pp. 197–205, 2007, doi: 10.1109/TEC.2006.889619.

[54] T. Boutsika and S. Santoso, "Quantifying Short-term Wind Power Variability," pp. 1–7, 2011.

[55] H. Holttinen, M. Milligan, B. Kirby, T. Acker, V. Neimane, and T. Molinski, "Using Standard Deviation as a Measure of Increased Operational Reserve Requirement for Wind Power," *Wind Eng.*, vol. 32, no. 4, pp. 355–377, 2008.

[56] M. Milligan *et al.*, "Operating Reserves and Wind Power Integration : An International Comparison," in *The 9th Annual International Workshop on Large-Scale Integration of Wind Power into Power Systems as well as on Transmission Networks for Offshore Wind Power Plants Conference Québec, Canada; October 18-19, 2010*, 2010, no. October.

[57] A. S. Brouwer, M. Van Den Broek, A. Seebregts, and A. Faaij, "Impacts of large-scale Intermittent Renewable Energy Sources on electricity systems, and how these can be modeled," *Renew. Sustain. Energy Rev.*, vol. 33, pp. 443–466, 2014, doi: 10.1016/j.rser.2014.01.076.

[58] H. K. Ringkjøb, P. M. Haugan, P. Seljom, A. Lind, F. Wagner, and S. Mesfun, "Short-term solar and wind variability in long-term energy system models - A European case study," *Energy*, vol. 209, p. 118377, 2020, doi: 10.1016/j.energy.2020.118377.

[59] E. Ibanez, I. Krad, and E. Ela, "A Systematic Comparison of Operating Reserve Methodologies," 2014.

[60] G. Bel, C. P. Connaughton, M. Toots, and M. M. Bandi, "Grid-scale fluctuations and forecast error in wind power," *New J. Phys.*, vol. 18, no. 2, 2016, doi: 10.1088/1367-2630/18/2/023015.

[61] J. Shi, L. Wang, W. Lee, X. Cheng, and X. Zong, "Hybrid Energy Storage System (HESS) optimization enabling very short- term wind power generation scheduling based on output feature extraction," *Appl. Energy*, vol. 256, no. September, p. 113915, 2019, doi: 10.1016/j.apenergy.2019.113915.

[62]   M. S. Silva Pinto, M. S. S. Pinto, O. R. Saavedra, and O. R. Saavedra, "Power reserve dispatch to mitigate variability of generation output due to wind ramps," *2020 IEEE PES Transm. Distrib. Conf. Exhib. - Lat. Am. T D LA 2020*, 2020, doi: 10.1109/TDLA47668.2020.9326195.

[63]   K. T. Bradford, D. R. L. Carpenter, Jr., and B. L. Shaw, "Forecasting southern plains wind ramp events using the WRF model at 3-km," in *AMS Student Conference, Atlanta, Georgia*, 2010, vol. 128, no. 3, pp. 247–253, doi: 10.1016/0378-1097(95)00100-J.

[64]   A. Florita, B. M. Hodge, and K. Orwig, "Identifying wind and solar ramping events," *IEEE Green Technol. Conf.*, no. January, pp. 147–152, 2013, doi: 10.1109/GreenTech.2013.30.

[65]   M. S. Eltohamy, M. S. A. Moteleb, H. Talaat, S. F. Mekhamer, and W. Omran, "Power System Flexibility Metrics Review with High Penetration of Variable Renewable Generation," *Int. J. Inf. Technol. Appl.*, vol. 8, no. 1, pp. 21–46, 2019, [Online]. Available: https://www.paneurouni.com/wp-content/uploads/2017/03/ita_1_2019.pdf.

[66]   M. S. Eltohamy, M. S. A. Moteleb, H. Talaat, S. F. Mekhamer, and W. Omran, "Technical Investigation for Power System Flexibility," in *6th International Conference on Advanced Control Circuits and Systems (ACCS) & 2019 5th International Conference on New Paradigms in Electronics & information Technology (PEIT)*, 2019, pp. 299–309, doi: 10.1109/ACCS-PEIT48329.2019.9062862.

[67]   M. Cui, J. Zhang, C. Feng, A. R. Florita, Y. Sun, and B. M. Hodge, "Characterizing and analyzing ramping events in wind power, solar power, load, and netload," *Renew. Energy*, vol. 111, pp. 227–244, 2017, doi: 10.1016/j.renene.2017.04.005.

[68]   G. Ye, Z. Wang, Y. Yan, and Z. Li, "Data-Driven Stochastic Unit Commitment Optimization Considering Spatial Correlation of Wind Farms," *2020 5th Int. Conf. Power Renew. Energy, ICPRE 2020*, pp. 582–587, 2020, doi: 10.1109/ICPRE51194.2020.9233279.

[69]   B. S.Everitt and A. Skrondal, *The Cambridge Dictionary of Statistics*, Fourth edi. Cambridge University Press, 2010.

[70]   C. Mihai, I. Lepadat, E. Helerea, and D. Călin, "Load curve analysis for an industrial consumer," *Proc. 12th Int. Conf. Optim. Electr. Electron. Equipment, OPTIM*, no. 3, pp. 1275–1280, 2010, doi: 10.1109/OPTIM.2010.5510494.

[71]   B. Ela, E., Milligan, M., and Kirby, "Operating Reserves and Variable Generation," *Natl. Renew. Energy Lab.*, no. NREL/TP-5500-51978, pp. 1–103, 2011, doi: 10.2172/1023095.

[72]   G. E. Corridors, "Dimensioning of Control Reserves in Southern Region Grid States," New Delhi, 2020.

[73]   A. Muzhikyan, A. M. Farid, and K. Youcef-Toumi, "An a priori analytical method for the determination of operating reserve requirements," *Int. J. Electr. Power Energy Syst.*, vol. 86, pp. 1–17, 2017, doi: 10.1016/j.ijepes.2016.09.005.

[74]   M. H. T. T. Thilekha *et al.*, "Impact of large-scale wind and solar power integration on operating reserve requirements of an Islanded power system," in *MERCon 2018 - 4th International Multidisciplinary Moratuwa Engineering Research Conference*, 2018, pp. 589–594, doi: 10.1109/MERCon.2018.8421919.

[75]   A. Abedi and M. Rahimiyan, "Day-ahead energy and reserve scheduling under correlated wind power production," *Electr. Power Energy Syst.*, vol. 120, no. March, p. 105931, 2020, doi: 10.1016/j.ijepes.2020.105931.

[76]   Y. Bapin and V. Zarikas, "Probabilistic Method for Estimation of Spinning Reserves in Multi-connected Power Systems with Bayesian Network-based Rescheduling Algorithm," in *the 11th International Conference on Agents and Artificial Intelligence (ICAART 2019)*, 2019, pp. 840–849, doi: 10.5220/0007577308400849.

[77]   Elia group, "Adequacy and flexibility study for Belgium 2020 - 2030," 2019. [Online]. Available: http://www.elia.be/~/media/files/Elia/publications-2/studies/20190628_ELIA_Adequacy_and_flexibility_study_EN.pdf.

[78]   W. Harvest, "Wind Farms in Belgium and Wind Speeds at known locations," 2020. https://windharvest.com/wp-content/uploads/2020/08/Belgium-Wind-Farms-with-15-and-20m-agl-wind-speeds-updated-8.7.20-1.pdf (accessed Sep. 29, 2021).

[79]   R. Brabant and R. Brabant, *Environmental Impacts of Offshore Wind Farms in the Belgian Part of the North Sea: Empirical Evidence Inspiring Priority Monitoring, Research and Management.*, no. January 2021. 2020.

[80]   R. Brabant, S. Degraer, and B. Rumes, "Offshore wind energy development in the Belgian part of the North Sea & anticipated impacts : an update," no. January, 2012.

[81]   WindEurope, "Wind energy in Europe 2020 Statistics and the outlook for 2021-2025." pp. 1–37, 2021, [Online]. Available: https://windeurope.org/intelligence-platform/product/wind-energy-in-europe-in-2020-trends-and-statistics/%0Afile:///C:/Users/kübra/Desktop/tezler/210224_windeurope_combined_2020_stats.pdf.

[82]   ELIA Group, "Belgium ' s electricity mix in 2020 : Renewable generation up 31 % in a year marked by the COVID-19 crisis," *Press Release*, no. January, pp. 1–7, 2021.

[83]   S. Le Bot *et al.*, "Optimal Offshore Wind Energy Developments in Belgium," 2004. [Online]. Available: http://www.belspo.be/belspo/organisation/publ/pub_ostc/cpen/rappcp21_en.pdf.

[84]   N. Akbari, D. Jones, and R. Treloar, "A cross-European efficiency assessment of offshore wind farms: A DEA approach," *Renew. Energy*, vol. 151, pp. 1186–1195, 2020, doi: 10.1016/j.renene.2019.11.130.

[85] A. Malvaldi, S. Weiss, D. Infield, J. Browell, and A. M. Foley, "A spatial and temporal correlation analysis of aggregate wind power in an ideally interconnected Europe," *Wind Energy*, vol. 20, no. March, pp. 1315–1329, 2017, doi: 10.1002/we.2095.

[86] A. Abedi and M. Rahimiyan, "Day-ahead energy and reserve scheduling under correlated wind power production," *Int. J. Electr. Power Energy Syst.*, vol. 120, no. February, p. 105931, 2020, doi: 10.1016/j.ijepes.2020.105931.

[87] L. Söder *et al.*, "Review of wind generation within adequacy calculations and capacity markets for different power systems," *Renew. Sustain. Energy Rev.*, vol. 119, no. October 2019, 2020, doi: 10.1016/j.rser.2019.109540.

[88] S. Van Ackere, G. Van Eetvelde, D. Schillebeeckx, E. Papa, K. Van Wyngene, and L. Vandevelde, "Wind Resource Mapping Using Landscape Roughness and Spatial Interpolation Methods," *Energies*, vol. 8, no. 8, pp. 8682–8703, 2015, doi: 10.3390/en8088682.

[89] "Elia, Belgium's electricity transmission system operator," 2021. http://www.elia.be/en/grid-data/power-generation/wind-power (accessed Jan. 31, 2021).

BIOGRAPHY OF AUTHORS

Mohammed Saber Eltohamy Research Assistant at Department of Power Electronics and Energy Conversion, Electronics Research Institute. He received the B.Sc. degree from the Faculty of Engineering at Shoubra, Benha University in 2004, and the M.Sc. degree in electrical engineering from Cairo University in 2014, and his Ph.D. degree from Ain Shams University, Cairo, Egypt in 2023. His research interests include Planning and Operation of Power Systems, Integration of Renewable Energy Systems, Distributed Generation, and Energy Management.
Email: mohammed_saber@eri.sci.eg

Mohammed Said Abdel Moteleb Professor at Department of Power Electronics and Energy Conversion, Electronics Research Institute. He received his B.Sc. And M.Sc. degrees from Cairo University, Cairo, Egypt in 1971 and 1978 respectively, and his Ph.D. degree from the Faculty of Electrical Engineering and information technology, Slovak Technology University, Slovakia in 1986. Prof. Moteleb is one of the leading editors-in-chief of the journal of electrical systems and information technology. His research interests include Control of Energy Systems and Optimization Techniques.
Email: moteleb@eri.sci.eg

Hossam E. A. Talaat Professor at the Electrical Engineering Department at Future University in Egypt. He was the former Head of the Electrical Power Engineering Department, Faculty of Engineering, Ain Shams University, Cairo, Egypt. He received his B.Sc. And M.Sc. degrees from Ain Shams University, Cairo, Egypt in 1975 and 1980 respectively, and his Ph.D. degree from the University of Grenoble, France in 1986. His research interests include Distributed Generation and Microgrids, Application of artificial intelligence techniques to Power System analysis, control, and protection; Real-time applications to electrical power systems and machines; Application of optimal and adaptive control techniques.
Email: hossam.eldeen@fue.edu.eg

Said Fouad Mekhamer received the B.Sc. degree in electrical engineering from Ain Shams University, Cairo, Egypt, in 1993, and the Ph.D. degree from the Dalhousie University, Canada, in 2002. He is currently a Professor at the Electrical Engineering Department at Future University in Egypt.
Email: said_fouad@eng.asu.edu.eg

Walid A. Omran received the B.Sc. and M.Sc. degrees in electrical engineering from Ain Shams University, Cairo, Egypt, in 1998 and 2005, respectively, and the Ph.D. degree from the Department of Electrical and Computer Engineering, University of Waterloo, Canada, in 2010. Currently, he is an associate professor at the German University in Cairo. His research interests include planning and operation of smart grids, integration of renewable energy systems and energy storage systems.
Email: walid.omran@fue.edu.eg